

# DYNAMIC SURFACE TENSION BEHAVIOR IN A PHOTORESPONSIVE SURFACTANT SYSTEM

Bradley A. Ciccirelli, Kenneth A. Smith, and T. Alan Hatton

Department of Chemical Engineering, Massachusetts Institute of Technology, Cambridge, MA 02139

**Abstract** - We report on the surface properties of a photoresponsive surfactant that incorporates the light-sensitive azobenzene group into its tail. *Cis-trans* photoisomerization of this group alters the ability of the surfactant to pack into adsorbed monolayers at an air-water interface or into aggregates in solution, causing a significant variation in bulk and surface properties upon changes in the illumination conditions. NMR studies indicate that a solution left in the dark for an extended period of time contains *trans* isomer almost exclusively, while samples exposed to light of fixed wavelength eventually reach a photostationary equilibrium with significant amounts of both isomers present. Dynamic surface tension studies performed on this system under different illumination conditions (dark, UV light, visible light) show profoundly different approaches to equilibrium. At concentrations well above the CMC, the same equilibrium tension is reached in all three cases, presumably corresponding to a surface saturated with the *trans* (more surface active) isomer. The dark sample shows a simple, single-step relaxation in surface tension after creation of a fresh interface, while the UV and visible samples exhibit a more rapid initial decrease in tension, followed by a plateau of nearly constant tension, and end with a final relaxation to equilibrium. It is hypothesized that this behavior of the UV and visible samples is caused by competitive adsorption between the *cis* and *trans* isomers present in these mixtures. Presumably the *cis* surfactant reaches the interface more quickly, leading to a *cis*-dominated interface having a tension value corresponding to the intermediate plateau, but is ultimately displaced by the *trans* isomer. Diffusional time scale arguments which consider the extremes of possible micellar dissolution rates are used to analyze the relaxation data of the dark sample, and the results indicate that micellar dissolution in these samples is slow.

**Index Terms** - azobenzene, competitive adsorption, dynamic surface tension, photoresponsive surfactants

## I. INTRODUCTION

The study of surface tension and other surface properties is motivated by the large number of industrially relevant processes involving interfaces, such as coating, detergency, printing, foams, etc. [1] These surface properties become increasingly important as the length scale of the system is reduced and the surface-to-volume ratio is increased (as in microfluidic devices). Many practical applications involve surfactant solutions and the creation of new interfaces on time scales smaller than those needed for the interfacial

properties to reach equilibrium values. In these cases, the dynamic interfacial properties have the most relevance. For this reason, dynamic interfacial phenomena have been the subject of much attention and research.

Recently, work has been done with surfactant systems which are responsive to a particular stimulus, such as light [2] or reduction/oxidation (redox) reactions [3]. These responsive surfactant systems allow for *in situ* and reversible control of many surfactant based properties [4], giving way to a variety of potential applications including controlled spreading and coating of surfaces, controlled release of substrates from micelles, and surface tension-driven (Marangoni) flows [5]. The ability to manipulate the surface activity and/or aggregation state of a surfactant system in a reversible fashion with spatial and temporal control has enormous potential. Light has an added advantage over other external stimuli in that it is non-invasive and easily focused and patterned. For example, the electrochemical approaches require that electrodes be inserted into the system and thereby restrict the possible range of experimental setups [2]. Focusing and patterning of light sources is easily achieved using optical lenses, filters, and masks.

The surfactant system studied here was first reported by Shang et al [6]. The surfactants are nonionic and feature the photoresponsive azobenzene group incorporated into the hydrophobic tail. As reported elsewhere [7, 8], azobenzene undergoes a reversible photoisomerization upon changes in illumination conditions. The more thermodynamically stable state is the *trans* form, which has a flat planar structure, as shown in Figure 1. Illumination with ultraviolet light converts the azobenzene into a bent *cis* state, which reverts back to the *trans* form either under illumination with visible light or by removal from light for an extended period of time. With the azobenzene group present in the tail of the surfactant, bulk and surface properties of the system can be altered by changing the illumination conditions.

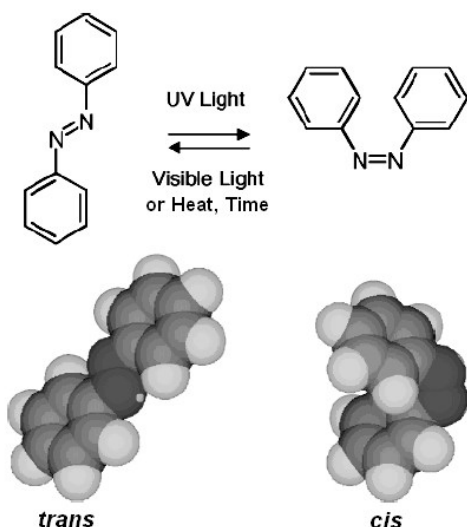


Fig. 1. Photoisomerization of azobenzene. Figure borrowed from Shang et al. [6].

## II. METHODS AND MATERIALS

### A. Materials

The surfactant used in these studies is di-ethylene glycol mono(4',4-hexyloxy, butyl-azobenzene) ( $C_4AzoOC_6E_2$ , hereon referred to as  $C_6$ ), shown in Figure 2. It was synthesized as described by Shang et al [6]

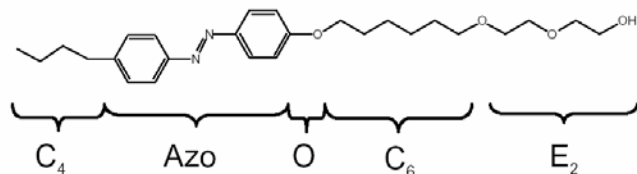


Fig. 2. Molecular structure of the photoresponsive surfactant  $C_4AzoOC_6E_2$ .  $C_4$  = butyl tail group; Azo = azobenzene group; O = ether oxygen middle polar group;  $C_6$  = alkyl spacer with 6 methylene groups;  $E_2$  = surfactant head group consisting of two ethylene oxide moieties. Figure borrowed from Shang et al. [6].

### B. UV-Vis

UV-Vis adsorption spectra were obtained on a Hewlett-Packard HP 8453 spectrophotometer.

### C. NMR

$^1H$  NMR scans were obtained at 500 MHz on a Varian instrument.

### D. Fluorescence

Fluorescence measurements were performed using a QuantaMaster spectrophotometer from Photon Technology International, Inc.

### E. Dynamic Surface Tension

Dynamic surface tension data were obtained using a

Krüss DSA10 drop shape analysis system. The profile of a pendant bubble of air submerged in surfactant solution contained in a quartz cuvette was tracked over time, and software performing axisymmetric drop shape analysis [9, 10] was used to determine a value of surface tension at each time increment. Optical filters were placed on the background light, as discussed later.

### F. Illumination

The light source used for illumination was a 200 W mercury lamp (Oriol 6283) mounted in an arc lamp housing (Oriol 66902) and powered by an arc lamp power supply (Oriol 68910). Visible light used for illumination passed through a 400 nm longpass filter (Oriol 59472), while a 320 nm bandpass filter (Oriol 59800) was used for UV light. Additionally, during dynamic surface tension measurements using the pendant bubble method, these filters were placed on the light source used for background light. In these experiments, a 750 nm bandpass filter (Oriol 57661) was used on background light for the dark samples. Characteristics of these optical filters can be seen in Figure 3.

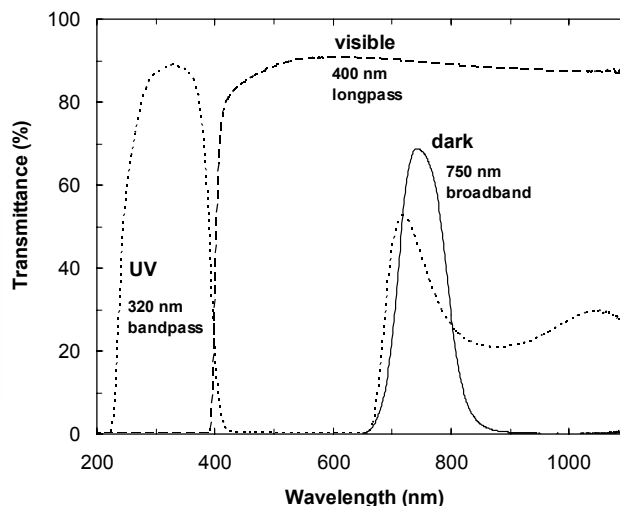


Fig. 3. Characteristics of the optical filters used during different experiments. The “visible” and “UV” filters were used to illuminate samples to photostationary states before making physical measurements. Additionally, these filters, including the “dark” filter were placed on background light during pendant bubble studies. (—) Dark filter. (---) Visible filter. (•••) UV filter.

## III. RESULTS AND DISCUSSION

### A. UV-Vis

The absorbance of aqueous solutions of  $C_6$  was measured with a UV-Vis spectrophotometer, and the results are shown in Figure 4. Measurements of the samples were taken under three different illumination conditions: first, measurements were taken after samples were removed from all light and kept in the dark for several days. Next, the samples were exposed to visible light using the optical filter shown in Figure 3.

Measurements were taken until the absorbance spectrum of the sample ceased to change appreciably upon further illumination, thus reaching a photostationary state [11]. Finally, samples were exposed to UV light (with filter shown in Figure 3) until a different photostationary state was reached.

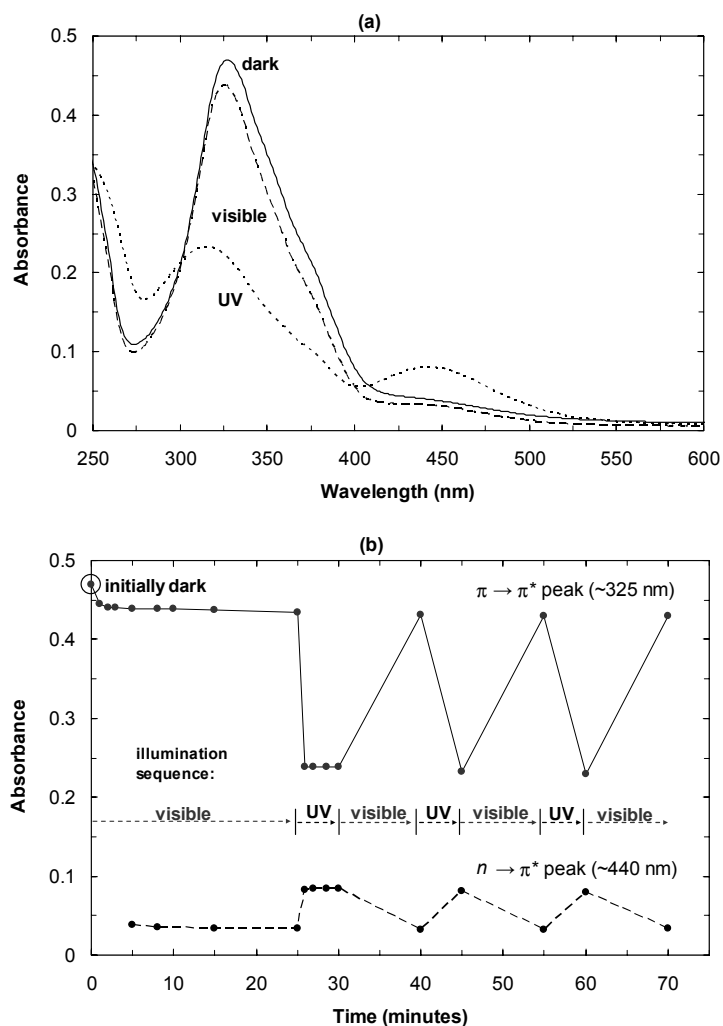


Figure 4. (a) Steady-state UV-Vis absorbance spectra for 0.03 mM  $C_6$  photosurfactant. (—) Dark sample. (---) Sample exposed to visible light. (•••) Sample exposed to UV light. (b) Transient behavior of UV-Vis absorbance peaks for 0.03 mM  $C_6$  surfactant originally in a dark state, then alternately illuminated with visible and UV light. (—) Absorbance peak near 320 nm. (---) Absorbance peak near 440 nm.

Figure 4a shows the spectra for the three states, with the “dark” curve representing the thermal equilibrium state reached after prolonged absence from light, and the “visible” and “UV” curves corresponding to the photostationary states reached after illumination with the appropriate filters. As reported earlier by Shang et al. [6], these surfactants show a strong absorbance band near 320 nm corresponding to a  $\pi$ - $\pi^*$  transition [11], with the visible and UV samples also showing an absorbance band near 440 nm corresponding to an  $n$ - $\pi^*$  transition. These peaks were tracked over time after increments of illumination, after starting with a dark sample, and the

results are shown in Figure 4b. 10 minutes of illumination using the Oriel lamp is found to be more than sufficient for the sample reach the visible photostationary state, while 5 minutes of illumination is more than enough to reach the UV photostationary state. Figure 4b illustrates the reversibility of the photoisomerization, as alternately illuminating the aqueous solutions with visible and UV lead to transitions back and forth between the two photostationary states.

### B. NMR

The isomeric composition of each of the illumination states was estimated from  $^1\text{H}$  NMR measurements [11]. In these studies, solid samples of surfactant were dissolved in deuterated chloroform ( $\text{CDCl}_3$ ) and then the scans were analyzed and the protons associated with each photoisomer were identified. Integration of these peaks allowed estimates of the *cis/trans* composition of each sample. The results indicated that sample in the dark state is almost exclusively (>99%) present in the *trans* form, while the two photostationary states contain mixtures of the two isomers (visible: 85-88% *trans*, UV: 10% *trans*). Ideally, deuterium oxide ( $\text{D}_2\text{O}$ ) would be used as the solvent in these experiments due to its similarity to water, but the extremely low critical micelle concentrations (CMCs) of these surfactants prevented such measurements from being practical.

### C. Fluorescence

Estimates of the CMC of this surfactant under the different illumination conditions were obtained using fluorescence measurements [12]. In these studies, a series of aqueous samples were prepared with varying surfactant concentration spanning two orders of magnitude. Additionally, each of these samples contained a fixed amount of the fluorescent probe Nile Red. Nile Red was chosen as the probe because its excitation peak occurs at a high wavelength ( $\sim 570$  nm) where absorption from the surfactant is minimal and because its emission is very environment-sensitive [13]. In hydrophobic domains, Nile Red fluorescence intensity is much greater than in aqueous domains. Thus, it is an appropriate probe for detecting the onset of micelles or other aggregates in solution. Each sample was excited with a 570 nm beam and the resulting fluorescent emission spectrum was measured. This measurement was performed on each sample for each of the three illumination states, and the peak intensities from the resulting emission spectra (which occur around 630 nm) are plotted against surfactant concentration as shown in Figure 5.

At low surfactant concentrations, the emission intensity is relatively low and is nearly identical for all illumination states. At the highest concentrations shown, where aggregates are present, the intensity is much greater and dependent upon the amount of hydrophobic domains present in solution, which differs between the different illumination states. With the low concentration data points

fit to a flat line of constant intensity and the high concentration points fit as a line with constant finite slope, the CMC for each illumination state can be estimated from the intersection of the extrapolated lines from the two regions. The results indicate that the CMC values for the dark, visible, and UV states are 1.1  $\mu\text{M}$ , 1.7  $\mu\text{M}$ , and 3.9  $\mu\text{M}$ , respectively. These extremely low CMC values illustrate the exceptional hydrophobicity of these surfactants, though the hydrophobicity lessens with increasing *cis* content. This is to be expected, as the *cis* isomer is known to have a higher dipole moment [6]. The CMC values obtained for the dark and UV states are in good agreement with those previously reported by Shang et al [6] for the “*trans*” and “*cis*” states, respectively.

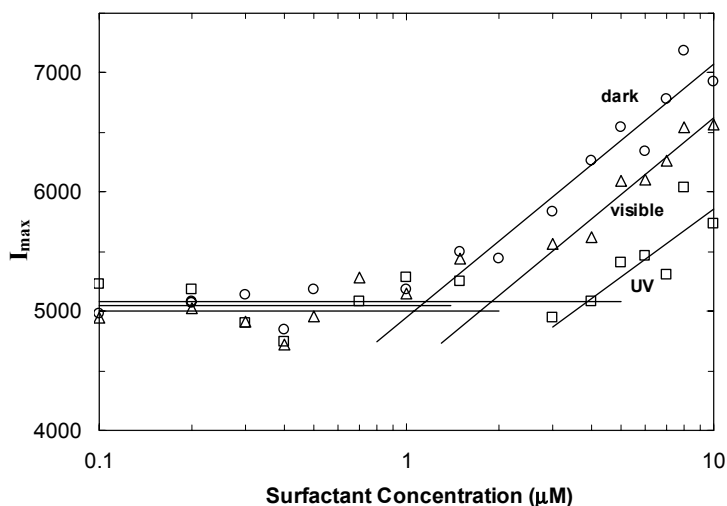


Fig. 5. Fluorescence emission peaks for solutions containing a fixed amount of Nile Red probe and varying amounts of  $C_6$  photosurfactant. (○) Dark sample. (Δ) Sample exposed to visible light. (□) Sample exposed to ultraviolet light.

#### D. Dynamic Surface Tension

The dynamic surface tension profile of these surfactants after the creation of a fresh air/water interface was measured by tracking the profile of a pendant bubble of air inside surfactant solution using axisymmetric drop shape analysis. These experiments require background light to sharpen the contrast between the disperse phase and the continuous phase [14], so for these studies, the optical filters shown in Figure 1 were placed on the background light source. For the visible and UV samples, this simply meant using the same filters that were used in illumination for driving conversion to the photostationary states. For the dark sample, a 750 nm broadband filter was used to allow light at a high wavelength where surfactant absorption is not appreciable. The results of these studies are shown in Figure 6. Due to the extremely low CMC values of these surfactants and the resulting impractical time scales needed for equilibration of interfacial properties, all dynamic surface tension measurements were performed at concentrations well above the CMC.

The curve for the dark sample is typical for these types of experiments: initially, when surfactant adsorption on the air/water interface is negligible, the surface tension remains high at a value near that of the pure solvent [15, 16]. As time passes and significant adsorption occurs, the surface tension decreases until eventually the interface becomes saturated with surfactant and the equilibrium surface tension is reached. The equilibrium surface tension found for the dark sample is in excellent agreement with the value previously reported for this surfactant in the “*trans*” state (29.5 mN/m) by Shang et al. [6] using the Wilhelmy plate method. The curves for the visible and UV samples, however, exhibit a rather different, interesting behavior. These curves show an intermediate plateau of nearly constant surface tension before ultimately reaching the same equilibrium tension as the dark sample. The surface tension value during this plateau is very near (and in the case of the UV sample, coincides with) the tension value (40.6 mN/m) identified by Shang et al. as the equilibrium value of the “*cis*” state. It is hypothesized that the behavior shown in the visible and UV states is due to competitive adsorption between the *trans* and *cis* isomers present in solution. This type of behavior has been reported for other systems containing mixtures of nonionic surfactants [17, 18]. Presumably, in these  $C_6$  samples the air/water interface is first dominated by *cis* surfactant, leading to the intermediate plateau in tension, but eventually becomes saturated with *trans* surfactant as the more surface active *trans* isomer reaches the interface and displaces the adsorbed *cis* surfactant.

Some interesting trends can be noted from these curves. First, in proceeding from dark to visible to UV, the CMC of the sample increases (as shown from the fluorescence measurements), and the initial decline in surface tension becomes more rapid, indicating an increase in the rate of transport of surfactant to the interface. Secondly, among the two photostationary state mixtures, the UV sample, which has the lower *trans* content, exhibits a longer intermediate plateau and takes much longer to finally reach the final equilibrium state. This is consistent with the competitive adsorption theory, which would indicate that the duration of the intermediate plateau and the time needed to reach the final *trans*-saturated equilibrium state would be limited by transport of *trans* surfactant to the interface. To further test this hypothesis, a mixture of the two photoisomers was created at a composition different from either of the photostationary state compositions. Dark and UV samples were mixed so as to create a solution with an estimated *trans* content of 50% (labeled “50/50” in the plots in Figure 6), and the “dark” filter was used on the background light during the pendant bubble experiments. As expected from its composition, which lies between the compositions of the visible and UV states, the 50/50 sample was intermediate between the visible and UV samples in terms of rapidity of initial surface tension decline, duration of the intermediate plateau, and the time needed to reach the final equilibrium.

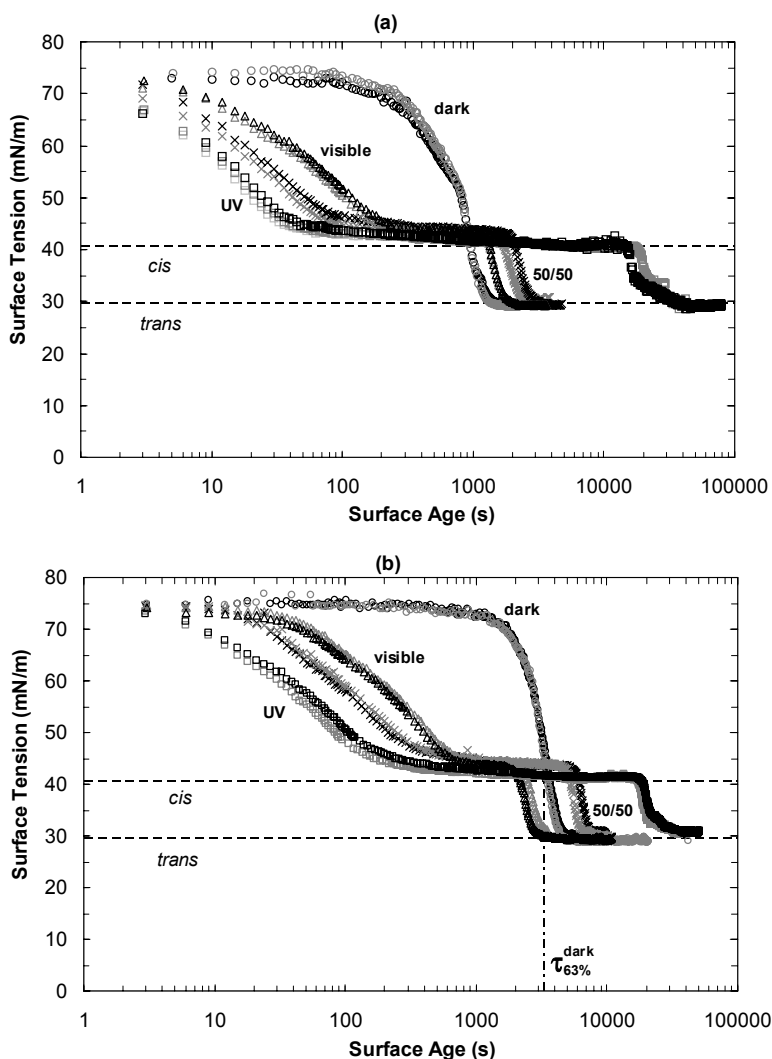


Figure 6. Dynamic surface tension profiles of  $C_6$  solutions under various illumination conditions obtained using the pendant bubble method. (○) Dark sample. (Δ) Sample exposed to visible light. (×) “50/50”: mixture of dark and UV samples designed to have equal amounts of *cis* and *trans* isomers present. (□) Sample exposed to UV light. Black and grey curves for each symbol indicate replicate experiments for the purposes of establishing reproducibility. Dashed lines labeled “*cis*” and “*trans*” correspond to equilibrium values reported by Shang et al [6]. (a) 0.191 mM  $C_6$  solution. (b) 0.04 mM  $C_6$  solution.

This raises an interesting subtlety in the data: the three isomer mixtures (visible, 50/50, and UV) have fairly disparate compositions (85-88%, 50%, and 10% *trans*), so when comparing data from the concentrations examined so far (in the range from 0.04 mM to 0.20 mM), the visible sample is always the first of the mixtures to reach the final equilibrium state, followed by the 50/50 sample and ultimately the UV sample. But when examining the dark and visible samples, which are closer in composition, the relative order in which they reach the final equilibrium depends upon the total surfactant concentration. Figure 4a shows that at 0.191 mM  $C_6$  concentration, the dark sample is actually the first to reach equilibrium, while in Figure 4b, at 0.04 mM, the visible sample actually reaches equilibrium first. Though not shown here, measurements

taken near 0.10 mM total  $C_6$  concentration indicate that this concentration seems to be the critical point at which the dark and visible reach equilibrium at the same time. This can be rationalized by considering the relative contributions of free monomers and aggregates to surfactant adsorption (the roles of aggregates will be discussed in greater detail in the next section). A simple comparison shows that, due to its higher CMC, a visible sample has more *trans* surfactant available as free monomer than a dark sample, even though a dark sample contains a greater total amount of *trans* surfactant (85% of 1.7  $\mu\text{M}$  is greater than 100% of 1.1  $\mu\text{M}$ ). So at lower total surfactant concentrations, where less surfactant is contained in aggregates, one can imagine that monomers play a larger role in adsorption than at higher concentrations when any additional surfactant present in solution is contained in aggregates. Thus, at 0.04 mM, monomer contributions to adsorption are important enough that transport of *trans* surfactant to the interface is greater in visible samples than in dark samples. While in the case of the 0.191 mM samples, aggregates play a greater role in transporting surfactant to the interface, and the dark state is able to saturate the interface with *trans* surfactant before the visible state. And apparently around 0.10 mM dark and visible samples have nearly identical transport rates of *trans* surfactant. [Note: in making this argument, it is assumed that the monomer population in a visible sample is 85-88% *trans* isomer, while the NMR data only tells us that the total sample is comprised of 85-88% *trans*. While it is not known exactly how the two isomers partition between the aggregate and monomer phases, the argument used here still applies as long as the *trans* content of the monomer population of the visible state is greater than 65%. Also, it has been recognized that at these high surfactant concentrations, the free monomer concentration may not be identical to the CMC. Nonetheless, it is convenient to use the CMC value as an estimate of the monomer concentration, and it seems safe to suppose that a visible sample contains more monomeric *trans* isomer than a dark sample.]

### E. Diffusional Time Scale Models

It is helpful when interpreting this dynamic surface tension data to calculate the expected time scales for diffusion of surfactant to the interface. A pertinent length scale in these systems is the depletion thickness  $\ell$  defined by

$$\ell = \frac{\Gamma}{C} \quad (1)$$

where  $\Gamma$  is the surface coverage and  $C$  is the surfactant concentration [19]. Indeed, even at the lowest concentrations studied, the depletion layer is on the order of 0.1 mm, which is significantly smaller than either of the physical length scales present in the experiment: the bubble radius ( $\sim 1$  mm) and cuvette width ( $\sim 10$  mm). Thus, the depletion layer is the relevant length scale for diffusion calculations.

Defining the diffusional time scale  $\tau_D$  in the conventional manner, it is found that

$$\tau_D = \frac{\ell^2}{D} = \frac{\Gamma^2}{C^2 D} \quad (2)$$

where  $D$  is the surfactant diffusivity in solution. In pre-micellar systems, there is no ambiguity regarding the values of concentration and diffusivity to be used in Eq. (2), as all surfactant in solution is present as monomer. However, in micellar systems such as the system under study here, care must be taken in determining the appropriate values of concentration and diffusivity. Aggregates in solution play a role in surfactant adsorption both by diffusion and by dissolution. It is helpful to examine two extremes, in order to place bounds on the expected behavior in micellar solutions. The first is to consider the case of extremely slow micelle dissolution. In this case, the micelles are essentially “frozen” and there is no net monomer exchange between the micelles and the bulk solution. In this case, micelle diffusion is more important than micelle dissolution. Transport of surfactant to the interface therefore takes place via the parallel processes of monomer diffusion and micelle diffusion. Since the micelles themselves are not surface active, implicit in this model is the notion that once a micelle reaches the interface, all of the surfactant that it contains is available for adsorption. In this model, the monomer and micelle contributions can be determined separately.

$$\tau_D^{monomer} = \frac{\Gamma_\infty^2}{(CMC)^2 D_{monomer}} \quad (3)$$

$$\tau_D^{micelle} = \frac{\Gamma_\infty^2}{(C_T - CMC)^2 D_{micelle}} \quad (4)$$

In these models  $\Gamma_\infty$  is maximum surface packing parameter obtained from a Frumkin isotherm fit to the equilibrium surface tension data [19] (alternatively,  $\Gamma_{eq} = \Gamma_{CMC} = \Gamma_{sat}$  could be used),  $C_T$  is the total surfactant concentration in solution, and  $D_{monomer}$  and  $D_{micelle}$  are the diffusivities of the monomer and micelle, respectively. The overall diffusional time scale for this model then is given by

$$\tau_D^{overall} = \frac{1}{\frac{1}{\tau_D^{monomer}} + \frac{1}{\tau_D^{micelle}}} \quad (5)$$

The other extreme is concerned with the case of infinitely fast aggregate dissolution. In this case, aggregates break up to replenish the bulk solution as soon as it is depleted, so that effectively all of the surfactant in solution is available as monomer. In this case the diffusional time scale becomes

$$\tau_D = \frac{\Gamma_\infty^2}{(C_T)^2 D_{monomer}} \quad (6)$$

It is then interesting to examine how the experimentally observed surface tension relaxation time scales compare to these estimates. In the system studied here, the dark

tension relaxation curves are the only that correspond to a “clean” experiment for examination, in the sense that the samples are not mixtures of isomers, the relaxation curves do not display an intermediate plateau, and the aggregation state is well-characterized with a measured diffusivity [20]. In contrast, the UV samples are less straight-forward to interpret due to the mixture of isomers present, the presence of the intermediate tension plateau, and the fact that Cryo-TEM studies of UV samples at high concentration done by Shang reveal a bicontinuous structure having less clearly defined transport properties [20]. A comparison of the dark data to the diffusional models is shown in Figure 7. The experimental data points correspond to the time needed for the tension to complete  $(1-e^{-1})(100\%) = 63\%$  of its relaxation to equilibrium (this time is indicated in Figure 4b). In the models, the value of  $\Gamma_\infty$  used is  $8 \times 10^{-6}$  mol/m<sup>2</sup> (found by Shang et al. for this surfactant [6]),  $D_{monomer}$  is  $5 \times 10^{-10}$  m<sup>2</sup>/s (typical monomer diffusivity reported in the literature [19]), and  $D_{micelle}$  is  $2.6 \times 10^{-12}$  m<sup>2</sup>/s (measured for this surfactant using dynamic light scattering at 0.10 mM [20]). The experimental data lie much closer to the “frozen” micelle model, indicating slow aggregate dissolution rates.

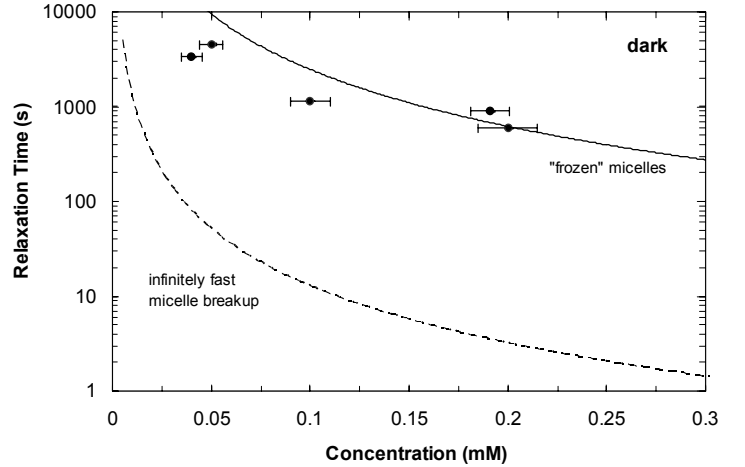


Figure 7. Characteristic tension relaxation times for dark  $C_6$  solutions of varying concentrations. Experimental points correspond to the time needed for the surface tension to complete 63% of its decline from initial value to equilibrium. This time is marked on Figure 4b. The dashed line corresponds to the diffusional time scale model calculated for the case of infinitely fast aggregate dissolution. The solid line represents the diffusional time scale model in which aggregate dissolution is considered to be extremely slow. In the models, the value of surface coverage used is the value reported by Shang et al. [6]:  $\Gamma_\infty^{trans} = 8.0 \times 10^{-6}$  mol/m<sup>2</sup>. The value of monomer diffusivity used is  $5 \times 10^{-10}$  m<sup>2</sup>/s [19]. The value of micelle diffusivity is  $2.6 \times 10^{-12}$  m<sup>2</sup>/s, which was found via light-scattering experiments for a 0.10 mM  $C_6$  solution under ambient light.

#### IV. CONCLUSIONS

We have reported on equilibrium and dynamic properties of a nonionic surfactant whose bulk and interfacial properties depend on the wavelength of light to which it is exposed. It is found that a solution of the surfactant that is left in the dark for an extended period of time contains only the *trans* isomer of the azobenzene

group incorporated into the tail, while sample exposed to light eventually reaches a photostationary state containing a mixture of the *cis* and *trans* isomers. It is also found that the CMC of a sample increases with its *cis* content. While all samples reach the same equilibrium state after creation of a fresh interface, the dynamic behavior of the surface tension during this relaxation is highly dependent upon the isomeric composition of the sample. Samples containing significant amounts of the *cis* isomer display an intermediate plateau of nearly constant tension before finally relaxing to equilibrium. The duration of this intermediate plateau and the time needed to reach the final equilibrium state are both dictated by the transport of *trans* isomer to the surface. It is hypothesized that this behavior is caused by competitive adsorption between *cis* and *trans* isomers present in solution, and that the intermediate plateau corresponds to a *cis*-dominated surface. The *cis* adsorbed on the surface is then eventually displaced by the more surface active *trans* isomer and the final equilibrium state reached by all samples corresponds to a surface saturated with *trans* surfactant.

Monomers and aggregates both contribute to adsorption, as indicated by the fact that the observed tension relaxation times decreased with increasing surfactant concentration, even when operating above the CMC. Furthermore, it seems that when comparing two samples and trying to predict which sample will reach the final equilibrium state first, one must consider both the isomeric composition and the total concentration (to determine the relative contributions of monomers and micelles). Analyzing relaxation data for dark samples in the context of diffusional time scale models indicates that aggregate dissolution in these samples is slow, and that the diffusion of the micelles is more important for adsorption than their dissolution.

These dynamic surface tension findings are significant because a number of photoresponsive surfactants have been synthesized and studied, and many of these systems exhibit mixtures of isomers/species under photostationary state conditions [2, 21-23]. The results reported here indicate that the presence of even a small amount of a second surface active species in solution can have a profound impact on the dynamic surface tension behavior of the system. Understanding the dynamic behavior of interfacial properties for these surfactants, particularly when mixtures are involved, and taking into account the role of aggregates in this behavior are crucial when considering applications for their use.

#### ACKNOWLEDGMENTS

This work was supported by the Singapore-MIT Alliance. B.A.C. is also grateful to Mr. Sanjoy Sircar for his help with NMR studies and Ms. Josephine Elia for her assistance in carrying out experiments.

#### REFERENCES

- [1] P. C. Hiemenz, Rajagopalan, R., *Principles of Colloid and Surface Chemistry*, 3rd ed. New York: Marcel Dekker, 1997.
- [2] J. Y. Shin and N. L. Abbott, "Using light to control dynamic surface tensions of aqueous solutions of water soluble surfactants," *Langmuir*, vol. 15, pp. 4404-4410, 1999.
- [3] B. S. Gallardo, K. L. Metcalfe, and N. L. Abbott, "Ferrocenyl surfactants at the surface of water: Principles for active control of interfacial properties," *Langmuir*, vol. 12, pp. 4116-4124, 1996.
- [4] B. S. Gallardo and N. L. Abbott, "In-Situ And Reversible Control Of The Assembly Of Redox-Active Surfactants In Aqueous-Solutions," *Abstracts Of Papers Of The American Chemical Society*, vol. 209, pp. 133-COLL, 1995.
- [5] D. E. Bennett, B. S. Gallardo, and N. L. Abbott, "Dispensing surfactants from electrodes: Marangoni phenomenon at the surface of aqueous solutions of (11-ferrocenylundecyl)trimethylammonium bromide," *Journal Of The American Chemical Society*, vol. 118, pp. 6499-6505, 1996.
- [6] T. G. Shang, K. A. Smith, and T. A. Hatton, "Photoresponsive surfactants exhibiting unusually large, reversible surface tension changes under varying illumination conditions," *Langmuir*, vol. 19, pp. 10764-10773, 2003.
- [7] T. Hayashita, T. Kurosawa, T. Miyata, K. Tanaka, and M. Igawa, "Effect Of Structural Variation Within Cationic Azo-Surfactant Upon Photoresponsive Function In Aqueous-Solution," *Colloid And Polymer Science*, vol. 272, pp. 1611-1619, 1994.
- [8] L. Yang, N. Takisawa, T. Hayashita, and K. Shirahama, "Colloid-Chemical Characterization Of The Photosurfactant 4-Ethylazobenzene 4'-(Oxyethyl)Trimethylammonium Bromide," *Journal Of Physical Chemistry*, vol. 99, pp. 8799-8803, 1995.
- [9] G. Faour, M. Grimaldi, J. Richou, and A. Bois, "Real-time pendant drop tensiometer using image processing with interfacial area and interfacial tension control capabilities," *Journal Of Colloid And Interface Science*, vol. 181, pp. 385-392, 1996.
- [10] B. H. Song and J. Springer, "Determination of interfacial tension from the profile of a pendant drop using computer-aided image processing. I. Theoretical," *Journal Of Colloid And Interface Science*, vol. 184, pp. 64-76, 1996.
- [11] H.-C. Kang, B. M. Lee, J. Yoon, and M. Yoon, "Synthesis and Surface-Active Properties of New Photosensitive Surfactants Containing the Azobenzene Group," *Journal of Colloid and Interface Science*, vol. 231, pp. 255, 2000.
- [12] K. P. Ananthapadmanabhan, E. D. Goddard, N. J. Turro, and P. L. Kuo, "Fluorescence Probes For Critical Micelle Concentration," *Langmuir*, vol. 1, pp. 352-355, 1985.
- [13] D. L. Sackett and J. Wolff, "Nile Red As A Polarity-Sensitive Fluorescent-Probe Of Hydrophobic Protein Surfaces," *Analytical Biochemistry*, vol. 167, pp. 228-234, 1987.
- [14] Krüss, "DSA1 v 1.80 Drop Shape Analysis Software User Manual." Hamburg, Germany, 2002.
- [15] H. Xi Yuan and M. J. Rosen, "Dynamic surface tension of aqueous surfactant solutions: I. Basic parameters," *Journal of Colloid and Interface Science*, vol. 124, pp. 652, 1988.
- [16] M. J. Rosen and X. Y. Hua, "Dynamic surface tension of aqueous surfactant solutions: 2. Parameters at 1 s and at mesoequilibrium," *Journal of Colloid and Interface Science*, vol. 139, pp. 397, 1990.
- [17] M. Mulqueen, K. J. Stebe, and D. Blankschtein, "Dynamic interfacial adsorption in aqueous surfactant mixtures: Theoretical study," *Langmuir*, vol. 17, pp. 5196-5207, 2001.
- [18] M. Mulqueen, S. S. Datwani, K. J. Stebe, and D. Blankschtein, "Dynamic surface tensions of aqueous surfactant mixtures: Experimental investigation," *Langmuir*, vol. 17, pp. 7494-7500, 2001.
- [19] J. K. Ferri and K. J. Stebe, "Which surfactants reduce surface tension faster? A scaling argument for diffusion-controlled adsorption," *Advances In Colloid And Interface Science*, vol. 85, pp. 61-97, 2000.
- [20] T. Shang, "A New Class of Photoresponsive Surfactants," in *Department of Chemical Engineering*. Cambridge, MA 02139: Massachusetts Institute of Technology, 2005.
- [21] J. Eastoe, M. S. Dominguez, P. Wyatt, A. Beeby, and R. K. Heenan, "Properties of a stilbene-containing gemini photosurfactant: Light-

triggered changes in surface tension and aggregation," *Langmuir*, vol. 18, pp. 7837-7844, 2002.

- [22] C. T. Lee, K. A. Smith, and T. A. Hatton, "Photoversible viscosity changes and gelation in mixtures of hydrophobically modified polyelectrolytes and photosensitive surfactants," *Macromolecules*, vol. 37, pp. 5397-5405, 2004.
- [23] C. T. Lee, K. A. Smith, and T. A. Hatton, "Photocontrol of protein folding: The interaction of photosensitive surfactants with bovine serum albumin," *Biochemistry*, vol. 44, pp. 524-536, 2005.